

Project Title:

Simulation and design of a transportable and compact neutron source based radiography system for industrial applications

Name: Sheng Wang

Laboratory at RIKEN: Neutron Beam Technology Team

1. Introduction

In order to generate high neutron fluxes to accommodate more scientific applications, high-power spallation sources, such as the ISIS, J-PARC, and SNS facilities have been realized [1]. An even more powerful source, the European Spallation Source (ESS), is currently under study [2]. However, since the primary mission of the high-power neutron sources is to serve a large number of users for materials characterization, and it is not cost-effective to use such expensive facilities for education and training or for evaluation of instrumentation ideas [3]. Employing low-energy protons on low-Z targets (e.g., Li, Be), as compared to high-energy protons on spallation targets (e.g., Ta, Hg), permits the use of compact accelerator-driven neutron sources (CANS). The CANS, due to their modesty in scale and capital/operation costs, and flexibility in instrumental configuration, are ideal to play a complementary role with respect to high-power neutron source. Therefore, the world community has increasingly recognized the value of CANS, and many CANS such as Low Energy Neutron Source (LENS) at Indiana University Cyclotron Facility (IUCF) of USA [4], RIKEN Accelerator-driven compact Neutron Source (RANS) in Japan as shown in Fig. 1, Compact Pulsed Hadron Source (CPHS) at Tsinghua University of China [5] and et al, have been constructed or under construction or under plan. An effective shielding design with compact size and low cost, as well as high safety is one of the most important issues for this kind of university scale neutron source.

Neutron Radiography (NR) is an important tool in non-destructive testing/inspection, which has been widely adopted in industrial, medical, metallurgical,

nuclear and explosive inspections. Inspection of ceramics or composite materials as well as detection of aluminium alloy corrosion damage is an example of effective applications for NR. Nuclear reactors supply high neutron fluxes and can be used to build up NR systems; nevertheless, the high technology involved, the costs and the impossibility of transporting them are limiting factors to the application and development of new fields of NR [6]. Alternatively, CANS can be used as neutron sources to generate NR images. In order to extend the application of the NR technique to a wider range, such as large industrial product like aircraft and ship, or infrastructure like bridges and buildings, it is necessary to design and construct transportable CANS systems for non-destructive testing/inspection. Such system must be lightweight and easy to operate, handle and repair. At the same time, it must be properly shielded.

Above all, to construct CANS, optimized shielding design is a very important issue, not only due to the consideration of safety and cost, but also the compact size and light weight, especially for the transportable neutron source development.

In this study, two CANSs were designed, i.e. a simple and easy-to-use small-scale neutron source at Kyoto University (KUANS), as well as RIKEN Accelerator-driven compact Neutron Source (RANS).

2. Simulation and design of KUANS

2.1. Configuration of KUANS target station

According to the mission of KUANS, the thermal neutron is what we need, and the fast neutron flux should be as small as possible to reduce the noise. Therefore the target station of KUANS was designed as a wing moderator configuration shown in Fig. 1.

Long life and reliable target design is a key factor for stable operation and performance of CANS. Thanks to the high neutron yield, high melting point, mechanical strength and stable performance, beryllium was used as KUANS's target. However, due to the problem of thermal damage and hydrogen embrittlement damage (blistering) on the beryllium target [5] [6], the target has to be maintained and replaced frequently. Recovery from any target failure takes many days: waiting for radiation decay, unstacking shielding, removing the highly radioactive target, cleaning the vacuum system, reassembling the system and waiting for vacuum recovery [6]. Hydrogen diffusible metal niobium was selected as target backing [7] and water as cooler for KUANS, as shown in Fig. 1. The combination of hydrogen diffusible metal and water cooling system provide a promising method to cope with the target damage problems for compact accelerator-driven neutron source.

2.2. Neutron and gamma source data for target

In this study, the neutron energy spectral distributions from the beryllium target for the incident proton energy of 3.5 MeV for $\theta=0-180^\circ$ (0° , 10° , 20° , 40° , 60° , 80° , 110° , 115° , 120° , 125° , 130° , 135° , 140° , 145° , 148°) were obtained by extrapolating the results of W. B. Howard et al measured at bombarding energies of 3.7 and 4.0 MeV [8]. The neutron energy spectrums of 0° , i.e., proton beam direction, for 3.5 MeV, 3.7 MeV and 4.0 MeV are shown in Fig. 2. According to M.R. Hawkesworth [9], the total neutron yield of proton with 3.5 MeV incident energy bombarding beryllium is 9.0×10^8 n/ μ C.

The measured ratio of gamma-ray to neutron yield for protons on beryllium at laboratory angle of 55° with less than 10% error is shown in Fig. 3 [10]. In the case of 3.5 MeV, the ratio is about 0.065. W. B. Howard et al [8] also measured the neutron yield for different solid angles in the case of 3.5 MeV proton energy. For 55° , it is about 5.9×10^7 neutrons/(sr μ C). So for proton it is about 3.8×10^6 photons/(sr μ C).

Under the assumption of isotropic angular distributions, the total photon yield can be obtained.

According to A. Z. Kiss, et al [11], photon is only generated from $^9\text{Be}(p,\alpha,\gamma)^6\text{Li}$ when ^9Be bombarded by proton with energy of 3.5 MeV, and the photon energy is 3.562 MeV.

2.3. Moderator simulation

Polyethylene was selected as moderator material for KUANS due to its excellent moderation effect. It has three parameters T1, T2 and T3 that have to be optimized as shown in Fig. 1 to get the thermal neutron flux as high as possible, while keeping the low ratio of fast neutron flux to thermal neutron flux. T1 is the distance from neutron emission surface S1 on the moderator to the nearest edge of the target, T2 is the thickness of moderator in proton beam direction, and T3 is the distance from the moderator surface S2 to the nearest edge of the target. The moderator surfaces S1 and S2 are displayed in Fig. 1. The thickness of moderator in neutron beam direction is the sum of T1, T3 and the target diameter. The thickness of moderator in the direction being perpendicular to the paper is kept the same as T2.

In this study, the thermal neutron is defined as the neutron with the energy from 1.0eV to 0.5eV, and its flux is checked at the detector which is put at 2m away from the target center. Furthermore, the collimator diameter is kept at 10cm. Figure 5 shows the thermal neutron flux with the variation of T1 and T2 under the condition of T3=2.5cm. From the figure, it is indicated that under the condition of same T1, with the increase of T2 thermal neutron flux increases at first, then decreases. The maximum value is obtained when T2 has same size with the collimator diameter, i.e., 10cm. From the figure, we also can see that the thermal neutron flux is sensitive to T1. For example, thermal neutron flux increases about 14% when T1 was changed from 2cm to -1.5cm under the condition of T2=12cm. Based on Fig. 5, the maximum thermal neutron flux for each T1 is extracted and displayed in Fig. 6. You can find

that the maximum thermal neutron flux can be obtained in the case of $T_1=1.5\text{cm}$ and $T_2=12\text{cm}$ (point with black circle in Figs. 5 and 6). According to the mission of KUANS, small ratio of fast neutron flux to thermal neutron flux is necessary. The ratios at two surfaces, i.e. neutron emission surface of moderator and detector surface at 2m away for the target center, were checked, and the results are displayed in Fig. 7 and Fig. 8, respectively. To have low fast neutron to thermal neutron ratio, while keeping high thermal neutron flux, $T_1=0.5\text{cm}$ and $T_2=12\text{cm}$ (point with red circle in Fig. 6) may be a good choice based on the two figures.

By fixing T_1 and T_2 , T_3 was varied from 1cm to 4cm. The thermal neutron flux is not sensitive to T_3 as shown in Fig. 9. For example, when T_3 increases from 1.5cm to 4cm, the thermal neutron flux only decreases about 2%.

Finally, the optimized moderator sizes may be: $T_1=0.5\text{cm}$, $T_2=12\text{cm}$ and $T_3=1.5\text{cm}$.

2.4. Reflector optimization

For reflector, there are five parameters, i.e. R_1 , R_2 , R_3 , R_4 and R_5 should be optimized. R_1 , R_2 , R_3 and R_4 are indicated in Fig. 1, and R_5 is the reflector thickness in the direction being perpendicular to the paper. As shown in Fig. 10, with the increase of reflector thickness, thermal neutron flux on the detector increases. But thermal neutron flux is only very sensitive to R_4 , for example, when R_4 increases from 3cm to 30cm, the thermal neutron flux increases about 27.4%. Considering the situation on-the-spot and effect of each side thickness of reflector to thermal neutron flux, an appropriate reflector parameter sizes may be: $R_1=13\text{cm}$, $R_2=5\text{cm}$, $R_3=5\text{cm}$, $R_4=20\text{cm}$ and $R_5=9\text{cm}$.

2.5. Shielding design

To make the shielding design compact, effective and low cost, borated polyethylene (BPE) with thickness of 50cm was put along the proton beam and neutron beam. Outside of BPE block, normal concrete was put as shown in Fig. 11. According to

the shielding simulation results in Figs. 12 and 13, along the neutron beam direction, both of neutron and gamma radiations are low, but in other directions, the neutron radiation is at the order of $103\mu\text{Sv}/100\mu\text{A/h}$, and the gamma radiation is about 102 to $103\mu\text{Sv}/100\mu\text{A/h}$. But since the accelerator-target complex of KUANS is in the shielded experimental hall and no one can have access to the room while beam is on, this radiation level can still be acceptable.

2.6. KUANS conclusions

In this paper, the design of target/moderator/reflector/shielding assembly of KUANS is introduced. The sizes of moderator and reflector were optimized with Monte Carlo code PHITS to have a high thermal neutron flux on the detector and keep the low ratio of fast neutron flux to thermal neutron flux. The optimized moderator sizes are: $T_1=0.5\text{cm}$, $T_2=12\text{cm}$ and $T_3=1.5\text{cm}$. The reflector can be designed as $R_1=13\text{cm}$, $R_2=5\text{cm}$, $R_3=5\text{cm}$, $R_4=20\text{cm}$ and $R_5=9\text{cm}$. The BPE and normal concrete are combined to shield neutron and gamma radiations. Although the radiations are high in the direction of backward direction of neutron beam, the current shielding design can still be acceptable since the operation room is different with the room where KUANS accelerator-target complex is put.

KUANS References

- [1] Filges and F. Goldenbaum, Handbook of Spallation Research, Wiley-VCH: Weinheim; 2009.
- [2] Andrew Taylor et al., A route to the brightest possible neutron source?, Science 2007; 315: 1092–1095.
- [3] C.-K, Loong, et al., The impact on science and technology of university-based, accelerator-driven, compact neutron and proton sources: A case in point in China, Physics Procedia 2012; 26 : 8-18.
- [4] T. Sato, et al., Particle and heavy ion transport code system PHITS, Version 2.52, J. Nucl. Sci. Technol. 2013; 50:9, 913-923.
- [5] T. Rinckel, et al., Target performance at the low

energy neutron source , Physics Procedia 2012; 26: 168-177.

[6] Xuewu Wang, Delivery of the first 3-MeV proton and neutron beams at CPHS : A status report on accelerator and neutron activities at Tsinghua University, Union of Compact Accelerator-Driven Neutron Sources IV, Hokkaido University, Japan, Sep., 24-27, 2013.

[7] Y. Yamagata, et al., Neutron source and its generation method, Patent 2012-049614 (in

Japanese).

[8] W. B. Howard et al, <http://www.nndc.bnl.gov>

[9] M.R. Hawkesworth, Atomic Energy Review 1977; 15 2: p. 169 .

[10] W. B. Howard et al, Measurement of the thick-target $\{sup 9\}$ Be (p, n) neutron energy spectra, Nuclear science and engineering 2001; 138:2.

[11] A. Z. Kiss, et al, Journal of Radioanalytical and Nuclear Chemistry 1985; 89: 123-141.

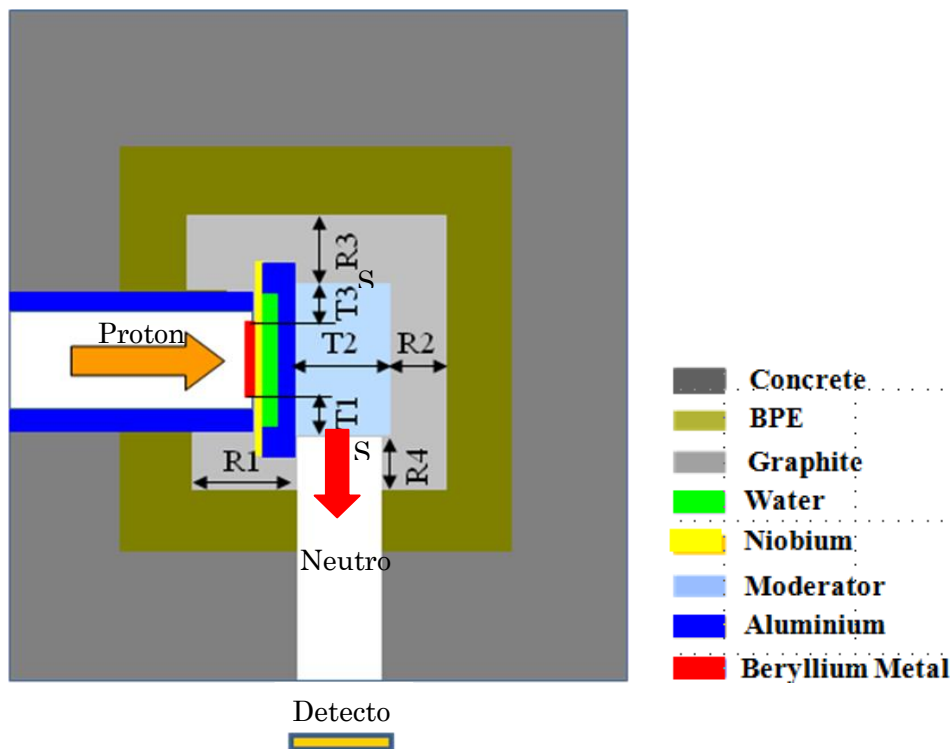


Fig. 1 Configuration of KUANS target station

RICC Usage Report for Fiscal Year 2014

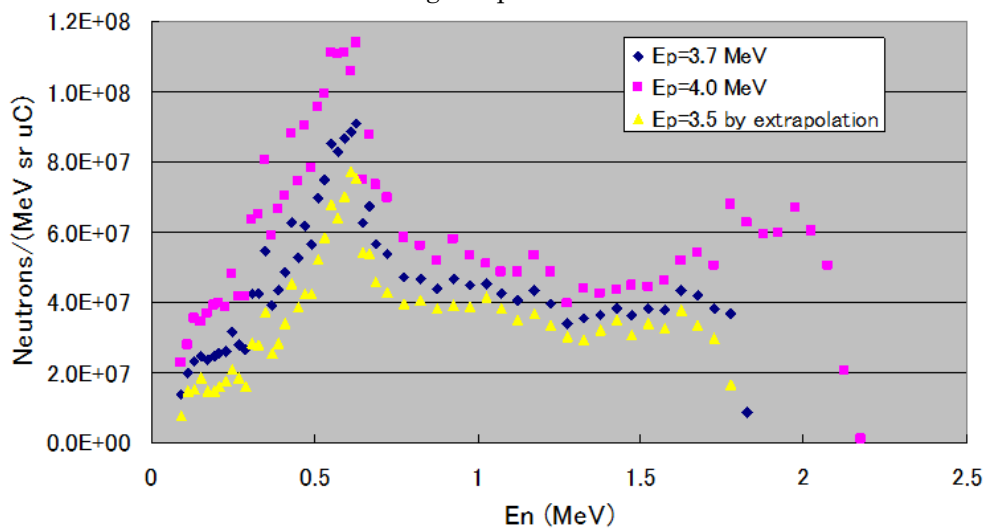


Fig. 2 Neutron energy spectrum at 0° for proton energy of 3.5 MeV, 3.7 MeV and 4.0 MeV

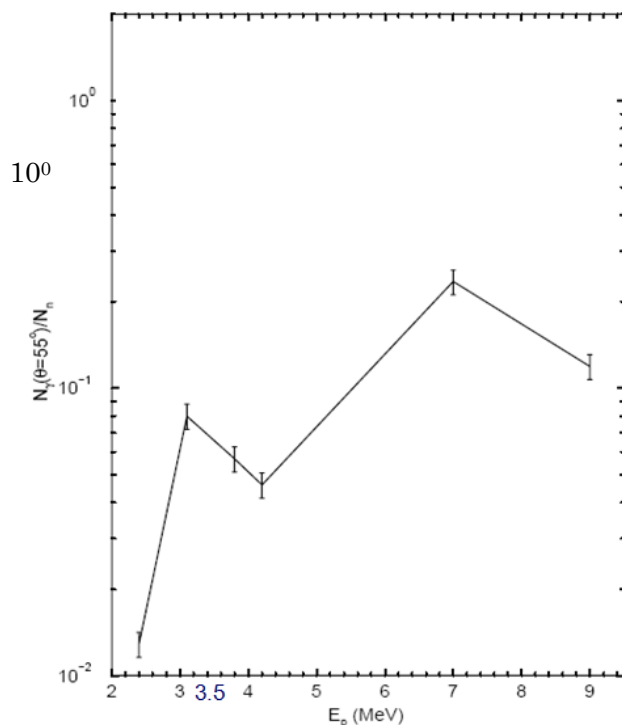


Fig.3 Ratio of photon to neutron yield at laboratory angle of 55o under different proton energies

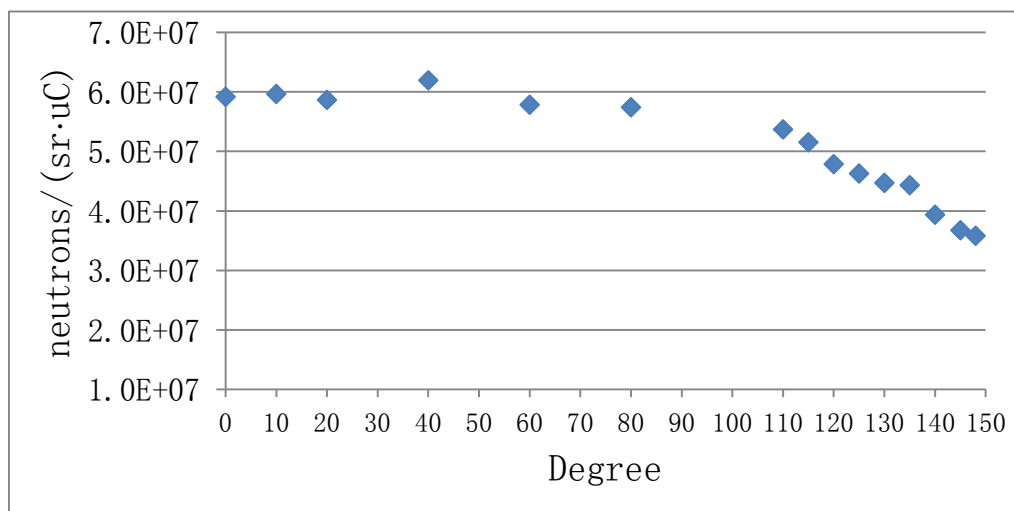


Fig. 4 Neutron yield under different laboratory angles for 3.5 MeV proton energy

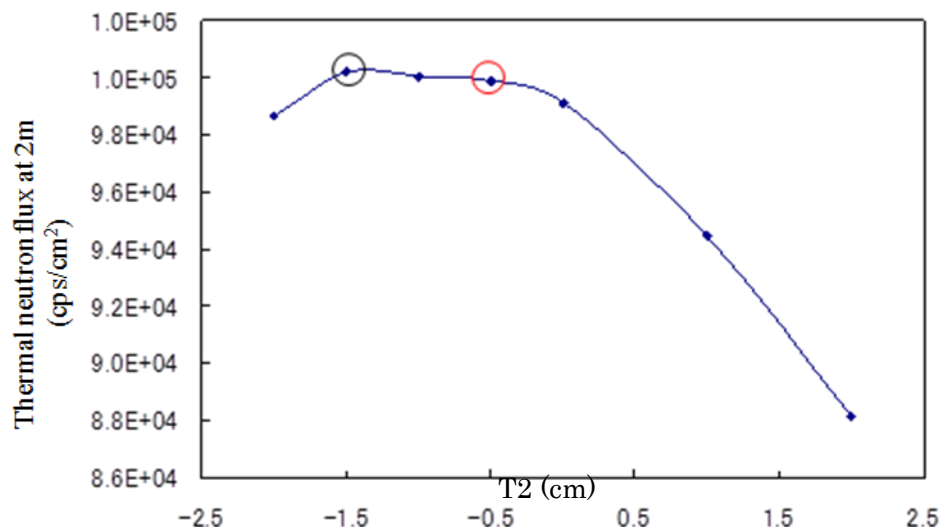


Fig. 5 Thermal neutron flux at 2m vs T2 under different T1

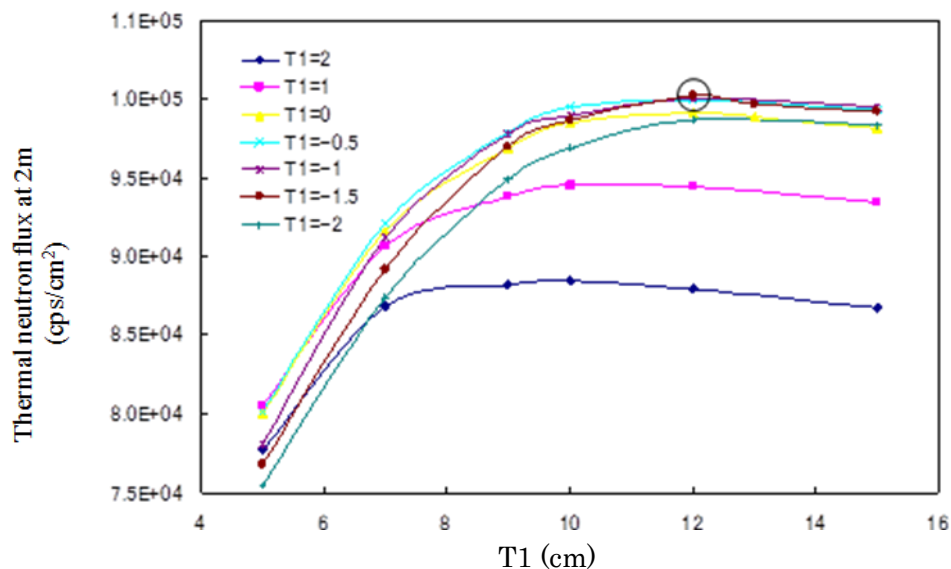


Fig. 6 Max. thermal neutron flux at 2m for each T1

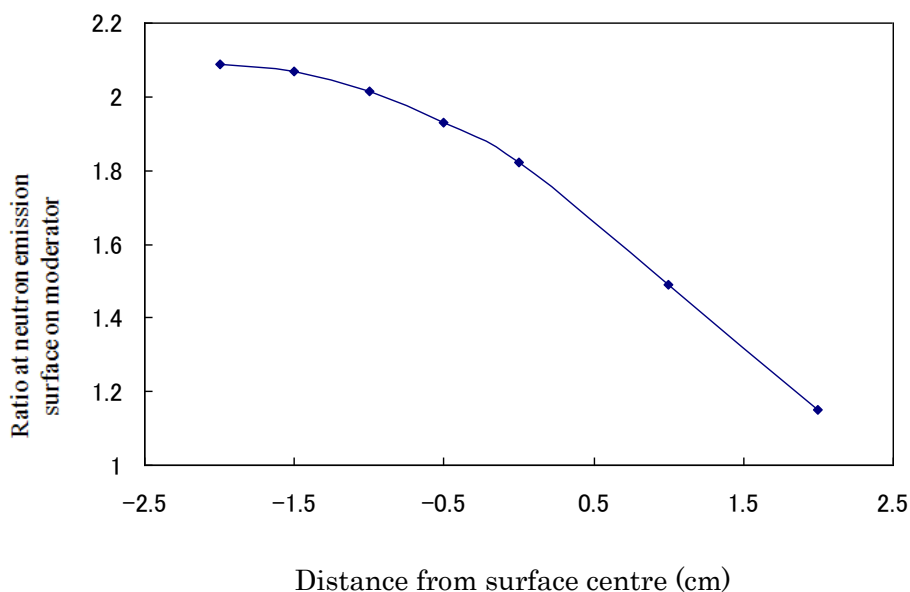


Fig. 7 Fast neutron to thermal neutron ratio on neutron emission surface of moderator

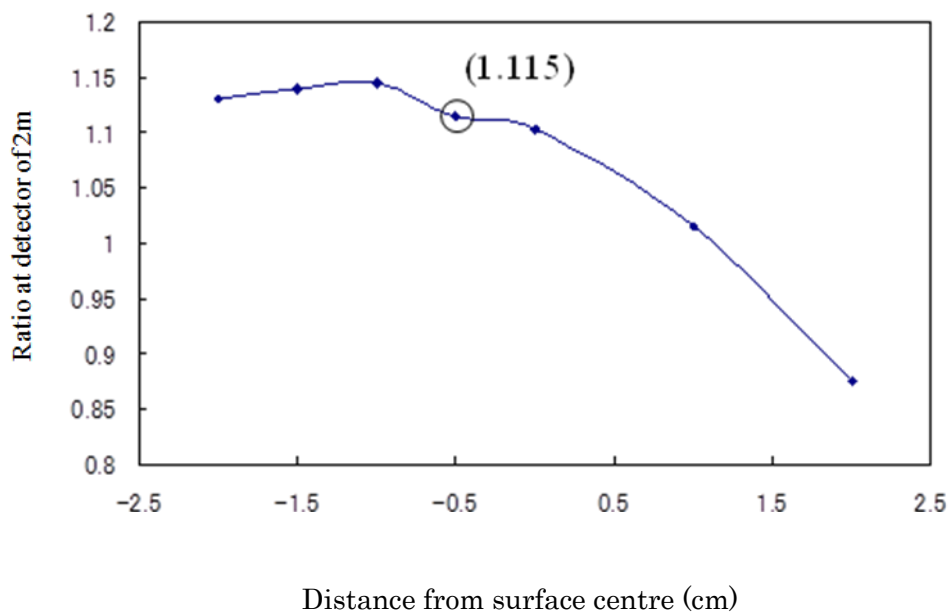


Fig. 8 Fast neutron to thermal neutron ratio on detector at 2m away from target centre

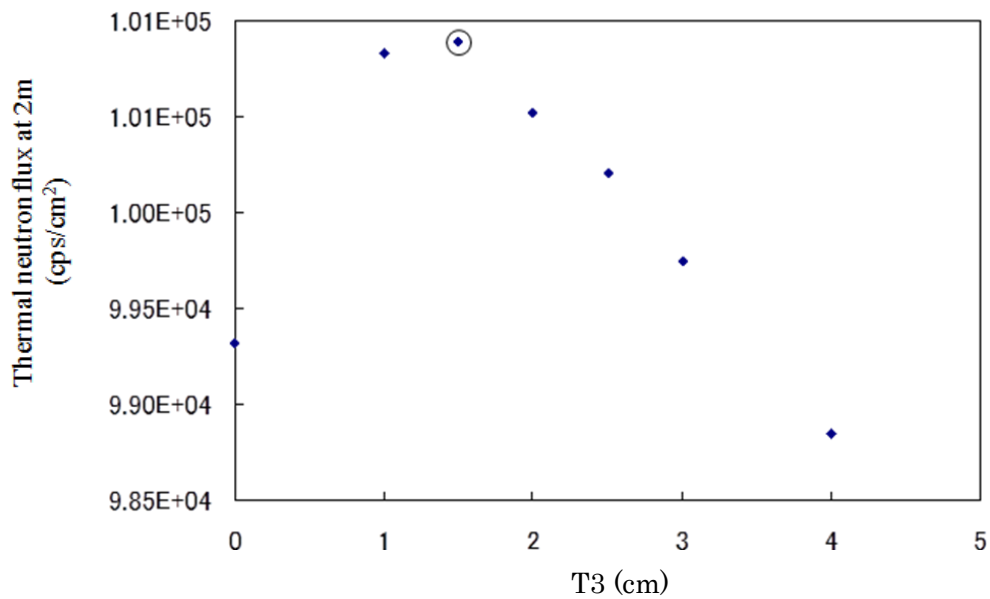


Fig. 9 Thermal neutron flux on detector at 2m away from target centre vs T3

3. Design and simulation of RANS

For RANS, two innovative shielding methods, i.e. multi-layer shielding design for target station and proton beam profile based shielding design to shield the backward neutrons from target, were proposed. Based on the operating conditions of a typical CANS, i.e. RANS, various materials available in marketing for the target station shielding design and for shielding the backward neutron in the proton tube were evaluated, and the advantage of two methods were verified via the quantitative analysis using Monte Carlo code PHITS [7] run on RIKEN Supercomputer RICC. The neutron and gamma dose equivalent rate of RANS were also measured and compared between measuring data and simulation results.

3.1 Innovative shielding methods and its application to RANS

3.1.1 Neutron shielding material evaluation for CANS target station

For the high flux neutron source, such as J-Park, concrete and steel are used as shielding material for target station. Although it has cost competitiveness, the necessity of heavy weight and big size is not suitable for the compactness demand of CANS, especially for the future transportable CANS. The energy of neutrons from the CANS target is around several MeV. Boron-10 is one of the elements that have the highest absorption cross section in the thermal neutron range, but the absorption cross section in fast neutron range is only about 1/5000 of the one in thermal neutron range. Therefore, to capture the neutron as much as possible, it is very important to reduce the neutron energy from fast level to thermal level. Light element, such as H-1 has very high scattering cross section. Due to the excellent mechanical and nuclear shielding characteristics of borated polyethylene (BPE), it is typically used in neutron shielding applications. The main function of polyethylene is to moderate the neutron energy, and then the neutron can be

absorbed by boron with high capture cross section. But depending on the neutron energy spectrum, the neutron shielding effect may be different for the BPEs with various ratios of boron concentration to polyethylene concentration. In this study, five types of BPE available in market [8] [9] are tested firstly according to the operating condition of RANS. The ratio of molar concentration for each BPE is shown in Table 1.

Figure 2 shows the typical target station configuration of CANS with slab system. Due to the high neutron yield, high melting point, mechanical strength and stable performance, beryllium is often used as CANS target. To solve the problem of hydrogen embrittlement damage and thermal damage on the target which has happened in LENS [10], hydrogen diffusible metal such as a thin plate of vanadium, and water cooler are combined with the target. Graphite is usually selected as reflector and polyethylene has excellent moderation performance to moderate the fast neutron to thermal neutron for thermal neutron radiography with CANS. Lead is usually used to shield the gamma. The thickness of neutron shield layer is 50cm for evaluating the shielding effect.

With the target station configuration shown in Fig. 2 and RANS's operation condition, i.e., 7MeV proton energy and the current of 100 μ A, the neutron shielding effect evaluations for BPE with different compositions have been carried out, and the neutron transmissions with the variation of BPE thickness are shown in Fig. 3. As indicated in this figure, the Material 1 in Table 1 has best neutron shielding performance.

Another neutron shielding material with high performance-to-price ratio is borated concrete [11], which has shown much better shielding performance than normal concrete and applied to the shield wall of the experimental room of the Versatile High Intensity Total Diffractometer of the J-PARC.

In this study, by taking the same configuration as in Fig. 2 and same operating condition as RANS, the

shielding effects of Model 1 BPE and the borated concrete for CANS target station were evaluated and compared. As indicated in Table 2, Model 1 BPE has better performance than the borated concrete. In addition to this, the BPE with density of 1.08 g/cm^3 is much lighter than the concrete with density of 2.2 g/cm^3 under the same size.

3.1.2 Multi-layer shielding design for target station

The CANS target will generate both neutron and gamma. Furthermore, a certain amount of gamma will also be generated during the neutron absorption. Therefore, the material to shield gamma should be put outside of neutron shielding material (e.g. BPE). Lead is the most effective and widely used gamma shielding material. But due to its high density and big size in the case of being outermost layer of target station, the CANS will be very heavy and also difficult to be constructed. To handle this problem, a multi-layer shielding design for target station is proposed, that is instead of putting one thick and heavy lead layer outside of one thick layer of BPE, one thin layer of lead will be inserted into BPE layer, and another thin layer will be put at outer of target station as shown in Fig. 3.

The CANS target will generate both neutron and gamma. A certain amount of gamma will also be generated during the neutron capture. Therefore, the material to shield gamma should be put outside of neutron shielding material. Lead is the most effective and widely used gamma shielding material. But due to its heavy density and big size in the case of being outermost layer of target station, the CANS will be very heavy and also difficult to be constructed. To handle this problem, a multi-layer shielding design for target station is proposed, that is instead of putting one thick and heavy lead layer outside of one thick layer of neutron shielding material, one thin layer of lead will be inserted into neutron shielding layer, and another thin layer will be put at outer of target station as shown in Fig. 4.

With RANS's operating condition, the neutron transmissions for target stations of single layer as

shown in Fig. 2 and multi-layer with same lead thickness and BPE thickness in Fig. 4 have been carried out. From the simulation results in Fig. 5 and Fig. 6, we can see that the multi-layer shielding design has better shielding effect than the single layer. In the case of multi-layer, gamma transmission rate of outermost layer is $4.13\text{E-}05$ and neutron transmission rate is $1.06\text{E-}07$, while for single layer gamma transmission rate is $4.48\text{E-}05$ and neutron transmission rate is $1.89\text{E-}07$. At the same time, by comparing with single layer shielding configuration, multi-layer one can save about 43% lead material, while keeping the similar amount of BPE material.

3.1.3 Proton beam profile based shielding method to shield backward neutrons from CANS target

Backward neutron from CANS target such as Be is usually strong. Shielding those neutrons is a knotty issue for CANS, since they have high energy and the geometry of accelerator DTL and RFQ are too complex to add some shielding materials outside of them. So in this study proton beam profile based shielding method was proposed. Again we take RANS operating conditions as example to show the effect of this method.

Figure 7 shows the simplified configuration of RANS. The left side in the figure is accelerator area and the right side is operating area. The space of the whole room (L x W x H) is $19.5\text{m} \times 11.4\text{m} \times 3\text{m}$ and surrounded by common concrete, except for the operating area side. The partition between the RANS and operating area is 0.5m thickness borated concrete of 3 segments as shown in the right side of Fig. 7. For the convenience of crane operation, there is 1m gap between the borated concrete wall and the ceiling.

Both of simulation and measurement have been carried out on RANS neutron and gamma dose equivalent rate distribution along the dot line in Fig. 7. Figure 8 (a) displays the measuring scene with neutron and gamma radiation measurement dosimeters. Due to the high radiation, the values

were read through web camera and display as shown in Fig. 8 (b). The measuring data and simulation result are shown in Fig. 8 and Fig. 9, respectively. From the two figures, we can see that the simulation result and measuring data have good agreement, and the radiation, especially neutron radiation is very high in accelerator side. The neutron dose equivalent rate in operating area is about 34 $\mu\text{Sv/h}$ and the gamma dose equivalent rate is about 5 $\mu\text{Sv/h}$, which are too high to be accepted for worker and researcher under long term operation. Various measures have to be taken to reduce the radiation, especially neutron radiation in accelerator side.

At first, BPE blocks with thickness of and length of were put along the proton tube shown in Fig. 11 and indicated as Case A. Proton beam profile of 7.0 MeV RANS Proton Linac was estimated by Trace3D and is shown in Fig. 11. According to the profile, the narrowest diameter of the profile is 3mm located in the position of 2.28m from the target. The diameter of proton tube is 60mm. Therefore, it is possible to put Chikuwa-shape shielding block inside the proton tube to shield backward neutron generated from the target.

Then based on Case A, BPE blocks are added in the end of proton tube as shown in Fig. 11 and it is indicated as Case B.

As shown in Fig. 13 of Case C, a Chikuwa-shape BPE block is put at the location of 2m from the target inside the proton tube based on the geometrical configuration of Case B. Its inner diameter is 2cm, so that proton beam can pass through it without any problem. In Case D, additional Chikuwa in the position of 55cm from the target is put based on Case C. The inner diameter of the Chikuwa is 3cm. The simulation results on one dimensional neutron equivalent dose distributions are displayed in Fig. 15. From this figure, it is clearly indicated that each neutron shielding measure is effective and finally the averaged neutron equivalent dose in operating area can be reduced from from 34.5 $\mu\text{Sv/h}$ of original one to 2.01 $\mu\text{Sv/h}$ of Case D as

shown in Table 3.

To make the shielding with Chikuwa shape block inside proton tube more effective, three neutron shielding materials, i.e., borated nitrogen with model of MBN-99, BPE and boron carbide (B4C) were employed and the shielding effects with the index of transmission rate are compared as shown in Fig. 16. In the range of low energy neutron, B4C has best shielding performance, and in the range of neutron energy with $\sim\text{MeV}$, both of B4C and BPE show good shielding effect. In total, the neutron transmission rate though MBN-99 block is 0.287, through BPE is 0.0965 and through B4C is 0.0741. So B4C is the most suitable neutron shielding material to be inserted into proton tube to shielding the backward neutrons.

3.3. RANS Conclusions

The value of CANS has increasingly recognized by the world community. An effective shielding design is one of the most important issues for RANS with compact size, low cost and high safety. In this study, the neutron shielding material suitable for CANS target station was investigated and BPE shows good performance. The multi-layer shielding design for CANS target station was proposed and may have better shielding effect and can save lead mass drastically by comparing with single layer target station under the conditional of same target station size. For CANS with beryllium target, the backward neutron flux from the target is high, which causes high neutron radiation level at operating area. After taking various measures in accelerator side, such as adding neutron shielding blocks along the outside of proton tube and inserting the Chikuwa-shape neutron shielding block into the proton tube based on the proton beam profile, the neutron equivalent dose can be reduced significantly at operating area. The evaluation of shielding design methods proposed in this study and neutron shielding effect estimation for different materials are based on the operating condition of a typical CANS i.e., RANS. The simulation results on one dimensional neutron and

RICC Usage Report for Fiscal Year 2014

gamma equivalent dose distributions have a good agreement with measuring data of RANS, which indicates the reliability of neutron shielding effect evaluation for different materials and shielding methods proposed in this study.

RANS References

- [1] Filges and F. Goldenbaum, Handbook of Spallation Research, Wiley-VCH (Weinheim, 2009).
- [2] A. Taylor, et al., Science 23, 1092, 2007. Andrew Taylor et al., "A Route to the Brightest Possible Neutron Source?" Science, Vol. 315, 23 February, 2007, pages 1092–1095.)
- [3] C.-K. Loong, et al., The Impact on Science and Technology of University-Based, Accelerator-Driven, Compact Neutron and Proton Sources: A Case in Point in China, Physics Procedia 26 (2012) 8-18.
- [4] C.M. Lavelle, et al., Neutronic design and measured performance of the Low Energy Neutron Source (LENS) target moderator reflector assembly, Nuclear Instruments and Methods in Physics Research A 587 (2008) 324–341.
- [5] Xuewu Wang, Delivery of the first 3-MeV proton and neutron beams at CPHS: A status report on accelerator and neutron activities at Tsinghua University, Union of Compact Accelerator-Driven Neutron Sources IV, Hokkaido University, Japan, Sep., 24-27, 2013.
- [6] A.X. da Silva, V.R. Crispim, Moderator-collimator-shielding design for neutron radiography systems using ^{252}Cf , Applied Radiation and Isotopes 54 (2001) 217-225
- [7] K. Niita, T.Sato, H.Iwase, H.Nose, H.Nakashima, L.Sihver, PHITS;a particle and heavy ion transport code system, Radiat. Meas., 41(2006)1080
- [8] <http://www.shieldwerx.com>
- [9] <http://www.askcorp.co.jp/>
- [10] T. Rinckel, et al., Target Performance at the Low Energy Neutron Source , Physics Procedia 26 (2012) 168 -177.
- [11] K. Okuno, et al., Development of novel neutron shielding concrete, Nuclear Technology, Vol 168, 2009

RICC Usage Report for Fiscal Year 2014



Fig. 1 Panoramagram of RANS (center: target station; right: proton Linac accelerator; left: beam dump)

Table 1 Ratio of molar concentration ratio for each BPE (%)[⊕]

Element Model	¹ H [⊕]	¹⁰ B [⊕]	¹¹ B [⊕]	¹² C [⊕]	¹⁶ O [⊕]
1 [⊕]	64.360 [⊕]	0.303 [⊕]	1.130 [⊕]	32.055 [⊕]	2.152 [⊕]
2 [⊕]	61.835 [⊕]	0.485 [⊕]	1.989 [⊕]	30.918 [⊕]	4.774 [⊕]
3 [⊕]	61.442 [⊕]	0.655 [⊕]	2.442 [⊕]	30.811 [⊕]	4.649 [⊕]
4 [⊕]	58.289 [⊕]	1.062 [⊕]	3.962 [⊕]	29.145 [⊕]	7.541 [⊕]
5 [⊕]	52.768 [⊕]	1.758 [⊕]	6.557 [⊕]	26.384 [⊕]	12.532 [⊕]

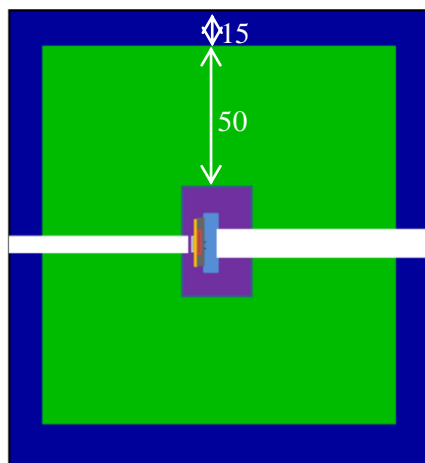


Fig. 2 Target station configuration of typical CANS with slab system

RICC Usage Report for Fiscal Year 2013

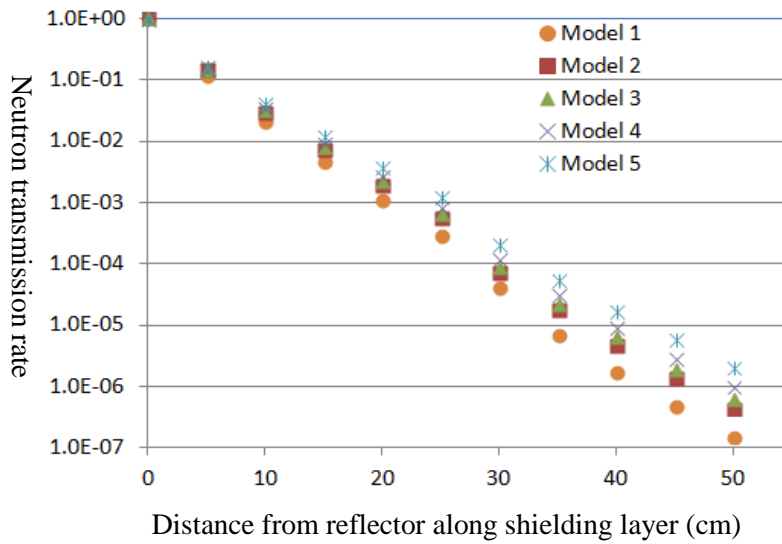


Fig. 3 Neutron transmission rate comparison for different BPE models

Table 2 Neutron transmission ratio comparison for BPE and borated concrete

Thickness Material	0	10	15	20	25	30	35	40	45	50
Model 1 BPE	1	2.18E-2	4.74E-3	1.15E-3	2.96E-4	8.01E-5	2.26E-5	6.64E-6	1.98E-6	5.87E-7
Borated concrete	1	2.44E-2	5.23E-3	1.25E-3	3.22E-4	8.65E-5	2.43E-5	7.08E-6	2.11E-6	6.27E-7

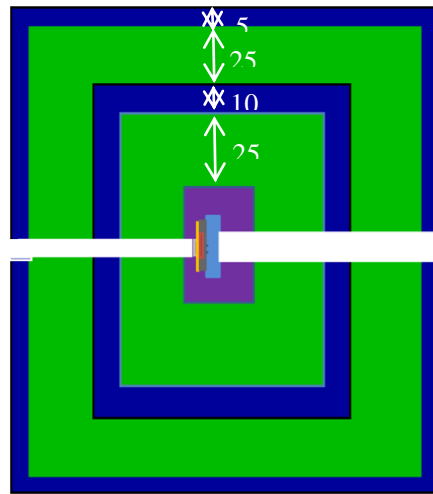


Fig. 4 Multi-layer CANS target station

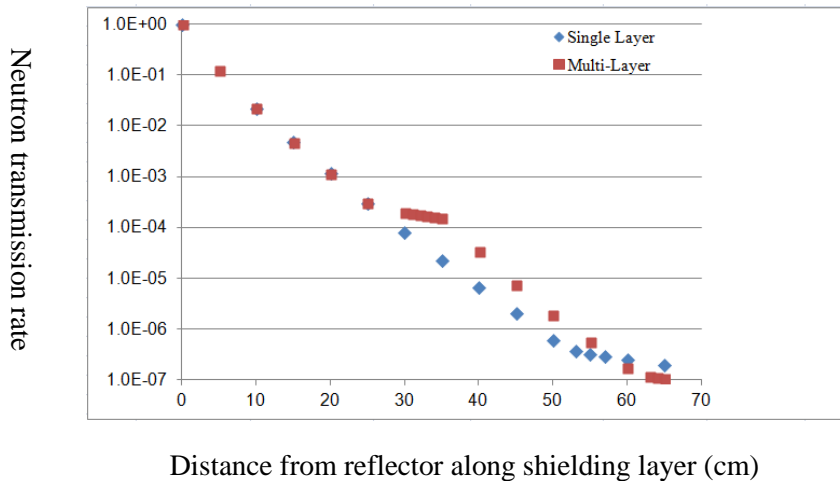


Fig. 5 Neutron transmission rate comparison between single and multi-layer shielding designs

RICC Usage Report for Fiscal Year 2013

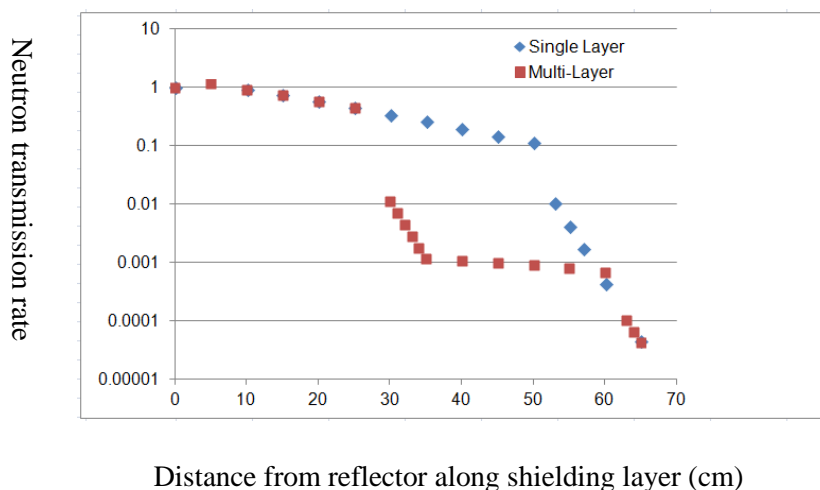


Fig. 6 Gamma transmission rate comparison between single and multi-layer shielding designs

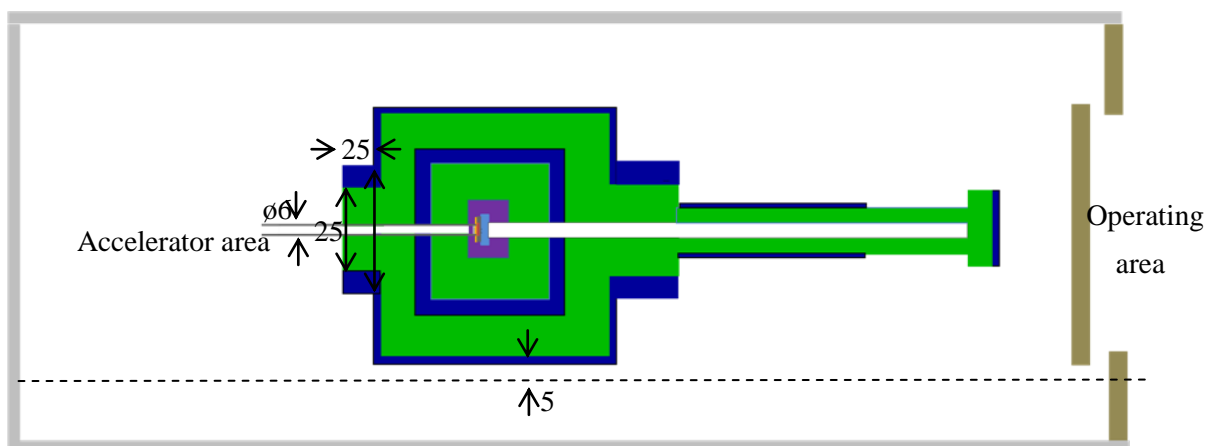


Fig. 7 Bird view of RANS with simplified configuration (cm)



Fig. 8 Scene of measurement (a. Neutron and gamma radiation measurements by dosimeters; b. Reading radiation value from display at operating area by using web camera)

RICC Usage Report for Fiscal Year 2013

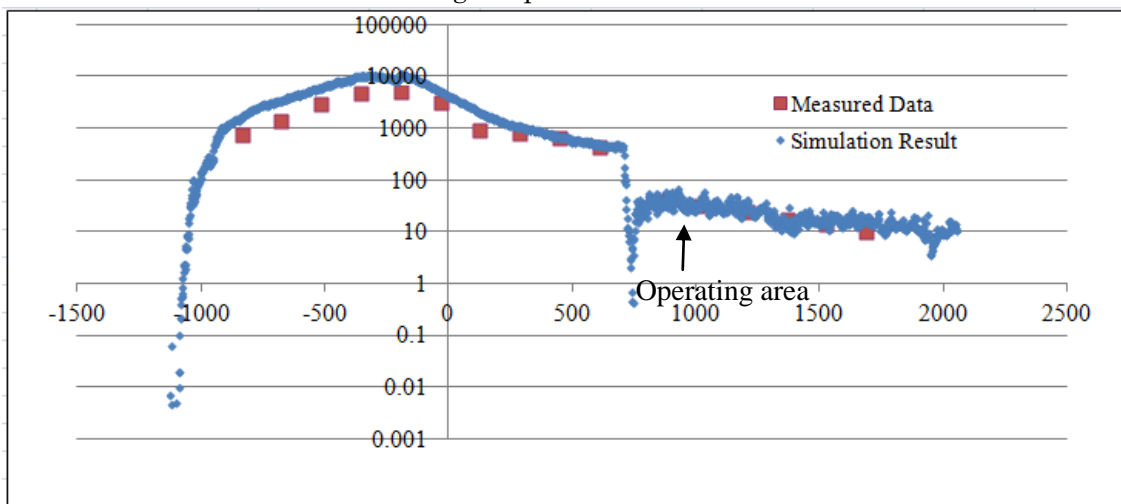


Fig. 9 Simulation and measurement data of one dimensional neutron radiation distribution

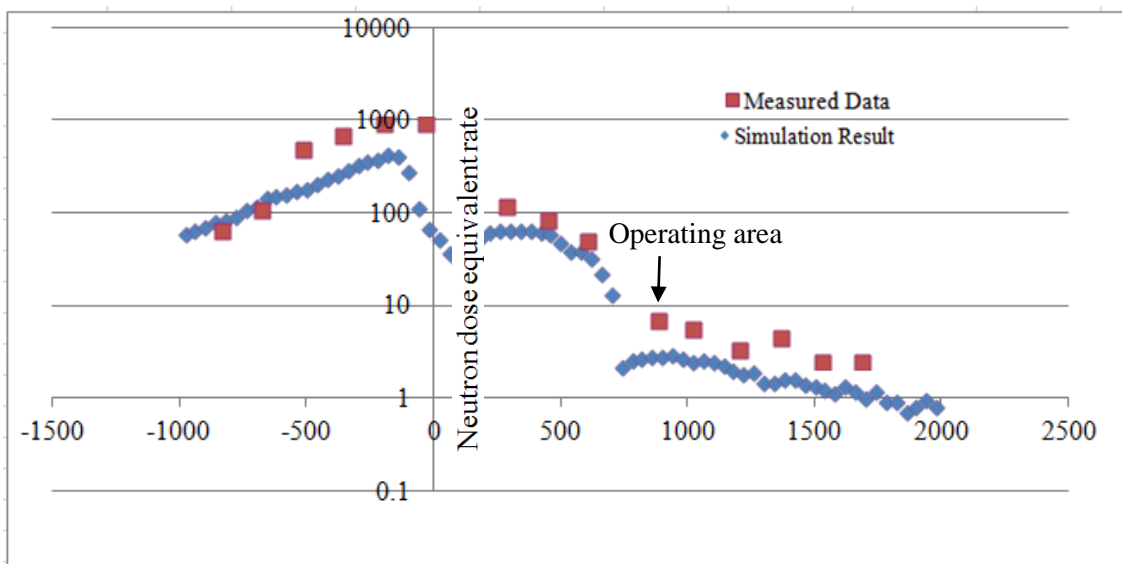


Fig. 10 Simulation and measurement data of one dimensional gamma radiation distribution

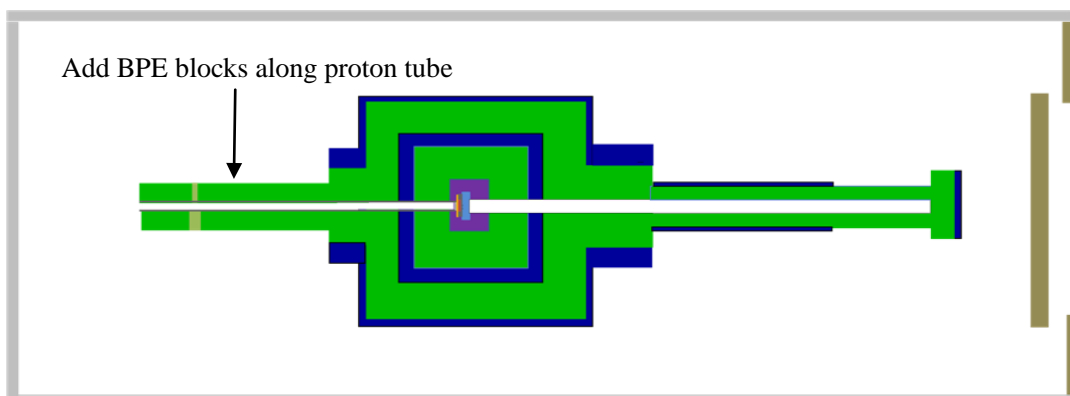


Fig. 11 Bird view of RANS with simplified configuration after adding BPE along outside of proton tube (Case A)

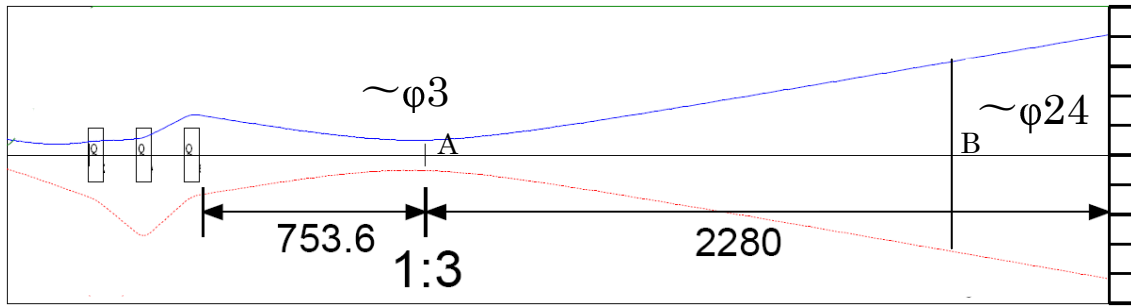


Fig. 12 Proton beam profile of RANS accelerator (mm)

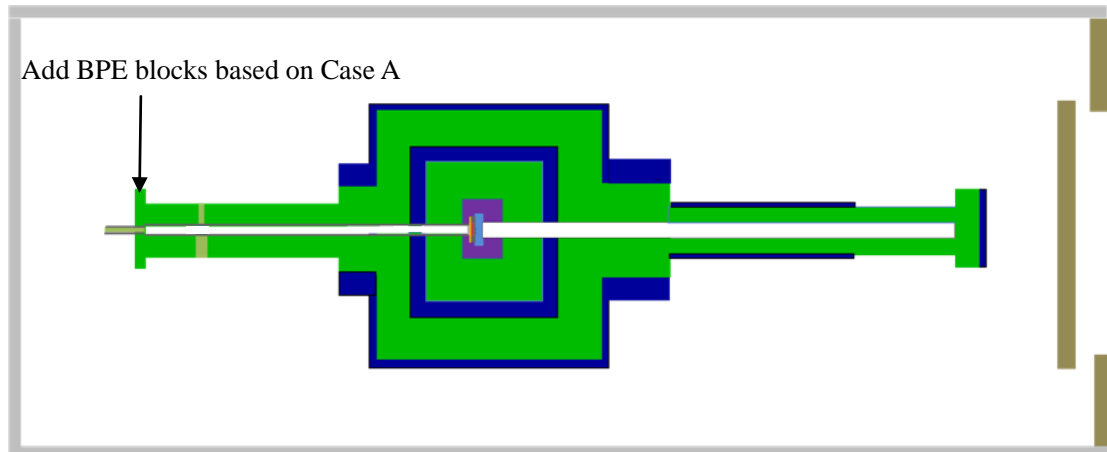


Fig. 13 Bird view of RANS with simplified configuration after adding BPE in the end of proton tube based on Case A (Case B)

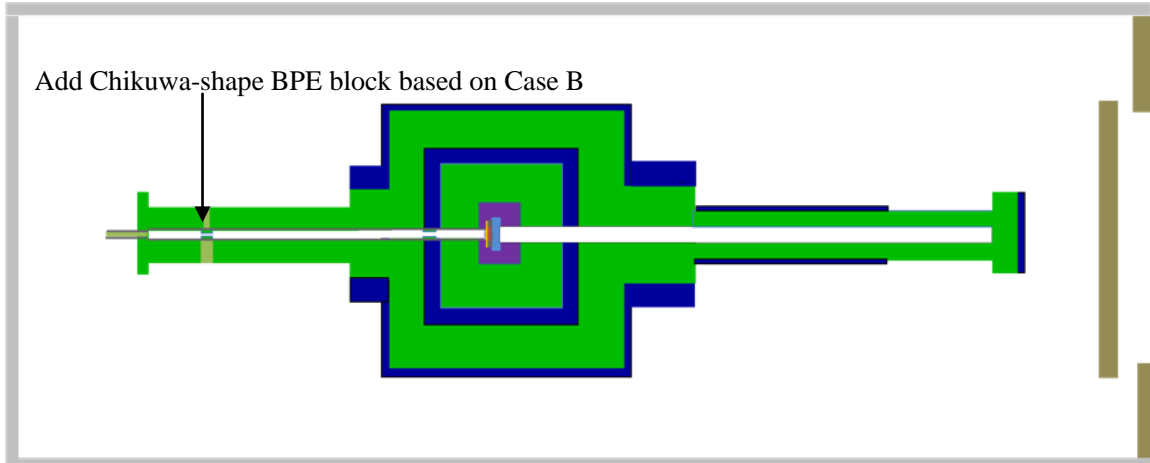


Fig. 14 Simplified bird view of RANS with Chikuwa-shape BPE blocks located in 2.0 m from target based on Case B (Case C)

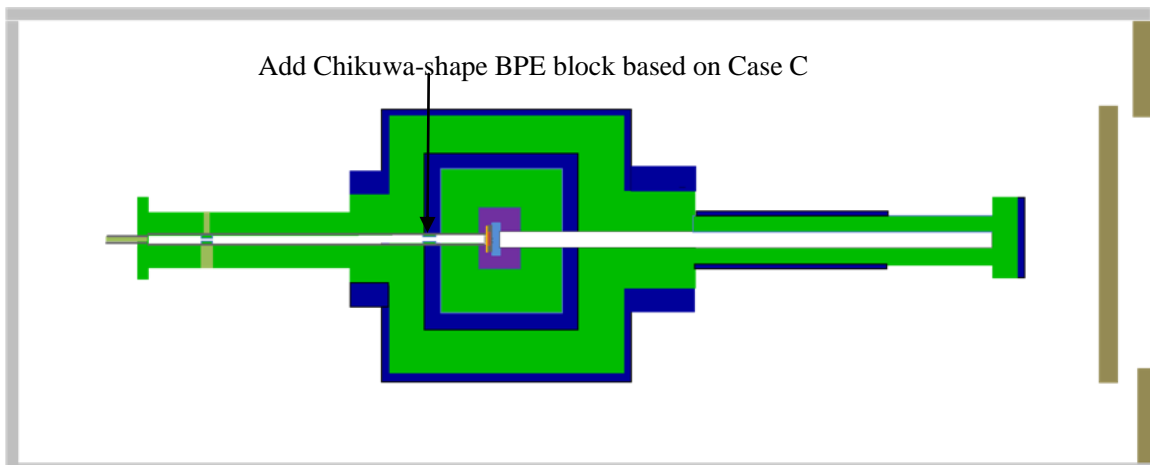


Fig. 15 Simplified bird view of RANS with Chikuwa-shape BPE blocks located in 55 cm from target based on Case C (Case D)

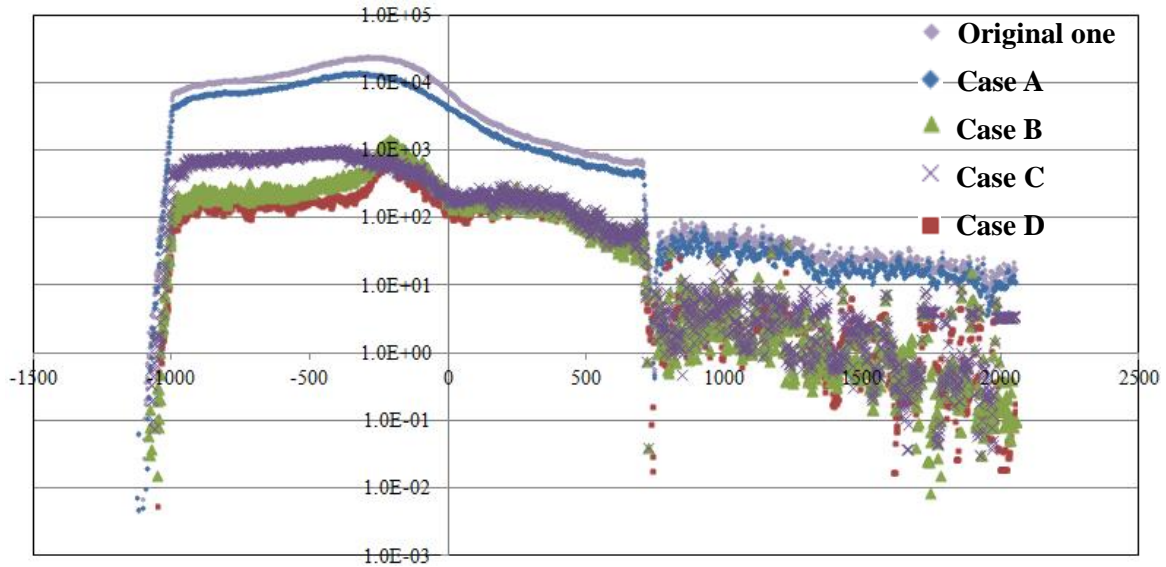


Fig. 16 One dimensional neutron equivalent dose distributions comparison among the original one and Case A to D

Table 3 Averaged neutron equivalent dose at operating area after taking various shielding methods

Case	Original	A	B	C	D
Neutron radiation ($\mu\text{Sv/h}$)	34.5	22.8	2.14	3.03	2.01

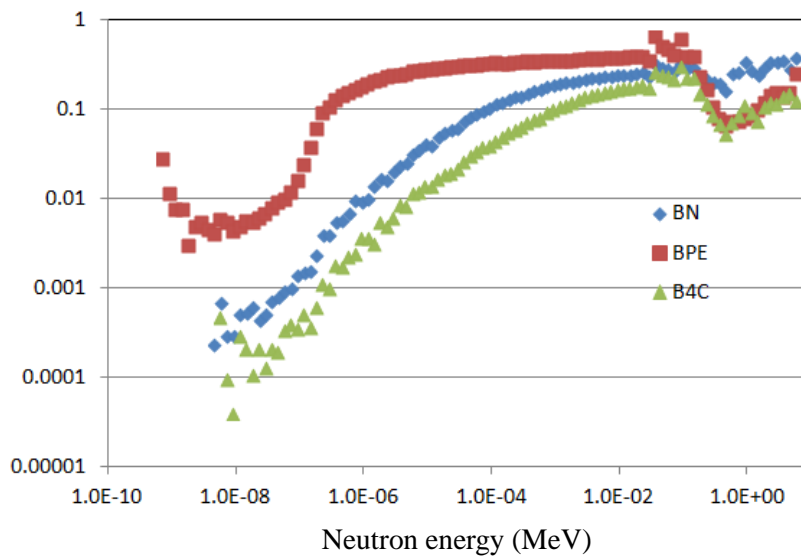


Fig. 17 Neutron attenuation rate comparison of different materials for Chikuwa shape block inside proton tube under different neutron energy

5. Schedule and prospect for the future

Within the fiscal year of 2015, the following three objectives have to be achieved with Monte Carlo simulation running on RICC. (1) Apr. 1, 2015-May 31, 2015: Complete the design for cold neutron beam line based on the RANS; (2) June 1, 2015-Oct. 31, 2015: Complete the novel moderator design; (3) Nov. 1, 2015-Mar. 31, 2016: Start an optimized design for fast neutron imaging system.

6. If you wish to extend your account, provide usage situation (how far you have achieved, what calculation you have completed and what is yet to be done) and what you will do specifically in the next usage term.

Up to now, we have reached to a new stage, i.e., RANS with thermal neutron beam line has been designed and constructed based on the Monte Carlo calculations using RICC. In the next usage term, a new cold neutron beam line will be designed on the RANS. After that, a new building for two compact neutron source facilities (3.9 MeV and 7.0 MeV) will be built in RIKEN Wako campus. Since the researcher and technical staff's office will be also in the same building, the radiation level must be very low and must be safe enough. Therefore, the shielding design for the two neutron source facilities and the building is very important and must be carried out carefully with Monte Carlo calculation by using RICC. Our final objective is to develop a transportable fast neutron imaging system. So after finishing the design for the two neutron source facilities and the building, optimized design for fast neutron imaging system will be started.

Fiscal Year 2014 List of Publications Resulting from the Use of RICC

[Publication]

1. Simulation and design of a simple and easy-to-use small-scale neutron source at Kyoto University, Sheng Wang, et al, Physics Procedia 60 (2014) 310 – 319.
2. Realization of the compact target station for the compact accelerator-driven neutron source at RIKEN, Sheng Wang, et al, submitted to NIMA.

[Oral presentation at an international symposium]

Shielding design of RIKEN Accelerator-driven Neutron Source (RANS), Sheng Wang, et al, 21st Meeting of International Collaboration on Advanced Neutron Sources, 29 Sep - 3 Oct 2014 in Mito, Ibaraki, Japan.